On the Effects of Rotating Gravitational Waves

J. Bičák*†‡, J. Katz†§ , T. Ledvinka* , and D. Lynden-Bell†

*Charles University, Prague †Institute of Astronomy, Cambridge, ‡Albert Einstein Institute, Potsdam, §The Racah Institute of Physics, Jerusalem

Introduction

It was just 100 years ago in Prague when Einstein wrote the paper [1] in which he, for the first time, expressed his understanding of Mach's Principle. Within his pre-General Relativity theory in which there was only one metric function he considered a mass point inside a shell accelerated "upwards" and found that the mass-point is dragged along by the shell.

Many formulations and studies of Mach's Principle appeared during the last 100 years, most of them were analyzed in the Tübingen conference in 1993 which led to the remarkable volume [2] containing lectures as well as valuable discussions. We studied Machian effects in various contexts, both in asymptotically flat spacetimes and within cosmological perturbation theory – see, e.g., [3], and number of references therein; later, cf. Schmid [4].

More recently, we investigated a subtle question whether dragging of inertial frames should be attributed also to gravitational waves. After the discovery of binary pulsars losing energy and angular momentum as a consequence of emitting gravitational radiation it would be surprising if gravitational waves did not have an influence on local inertial frames. However, there are still doubts uttered about the status of gravitational stress-energy as compared with stress-energy tensor $T_{\mu\nu}$ of matter in relation to Machian ideas (see, e.g., [2], p. 83).

In the present work [5] we investigate the effects of rotating gravitational waves in a more general, asymptotically flat setting, without assuming cylindrical symmetry. We again start out from linearized theory and construct an ingoing rotating pulse of radiation which later transforms into an outgoing pulse. While in the cylindrical case our waves were characterized by just one harmonic index m governing the number of wave crests in φ, now the situation becomes considerably richer involving both spherical harmonic indices l and m.

Near the origin the first-order metric of our waves behaves as r^l, so the region around the origin will be very nearly flat for l sufficiently large. When, however, a local inertial frame is introduced at the origin, we find that its axes rotate with respect to the lines $\varphi = \text{const}$ of the global frame, i.e., with respect to stars at infinity.

Near the origin the congruence of the worldlines $\varphi = \text{const}$ twists and the observers attached to these lines experience Euler acceleration proportional to $d_t\omega_0$, where ω_0 is the angular velocity of the inertial frame near the origin. The angular velocity ω_0 enters *the second-order odd-parity dipole $l = 1$ perturbation* of the metric, $g^{(2)}_{t\varphi} = -\omega_0\, r^2 \sin^2\theta$. (The Coriolis and centrifugal accelerations are higher order in the angular velocity.) The situation thus indeed resembles the interior of a collapsing slowly rotating shell - see [6] where the vorticity of the lines $\varphi = \text{const}$ is given in covariant form. In [6] we also calculated how the fixed stars at infinity rotate with respect to the inertial frame at the origin by considering photons emitted radially inwards from the stars.

Metric perturbations

We consider first the linearized theory of gravity in a flat background in spherical coordinates decomposing the metric perturbations into tensor harmonics [11], [12], [13]. For our purpose it is sufficient to consider odd-parity waves. We use the Regge-Wheeler gauge condition for odd-parity perturbations ($(i) = (1), (2)$ denotes the first- and second-order perturbations)

$$h^{(i)}_{\mu\nu} = \sum_{lm}\left[-\frac{\sqrt{2l(l+1)}}{r} h^{(i)}_{0lm}(t,r)c_{0lm\,\mu\nu} + i\frac{\sqrt{2l(l+1)}}{r} h^{(i)}_{1lm}(t,r)c_{lm\,\mu\nu}\right] \quad (7)$$

where c_{0lm}, c_{lm} are the odd-parity harmonics with explicit forms of the non-zero components

$$c_{0lm\,t\theta} = \frac{r}{\sqrt{2l(l+1)}}\frac{1}{\sin\theta}\partial_\varphi Y_{lm}, \quad (8)$$

$$c_{0lm\,t\varphi} = -\frac{r}{\sqrt{2l(l+1)}}\sin\theta\partial_\theta Y_{lm}, \quad (9)$$

$$c_{lm\,r\theta} = \frac{ir}{\sqrt{2l(l+1)}}\frac{1}{\sin\theta}\partial_\varphi Y_{lm}, \quad (10)$$

$$c_{lm\,r\phi} = -\frac{ir}{\sqrt{2l(l+1)}}\sin\theta\partial_\theta Y_{lm}, \quad (11)$$

Rotating scalar waves

For the scalar wave equation in spherical coordinates r, θ, φ

$$-\frac{\partial^2\psi}{\partial t^2} + \Delta\psi = 0 \quad (1)$$

we search for solutions in the form

$$\psi_{lm} = \text{Re}\, Q_l(t,r)Y_{lm}(\theta,\varphi), \quad (2)$$

where $Y_{lm} = N^m_l P^m_l(\cos\theta)e^{im\varphi}$, $\quad l \geq 0$, $\;|m| \leq l$ are scalar spherical harmonics, i.e. the radial part satisfies

$$-\ddot{Q}_l + Q''_l + \frac{2}{r}Q'_l - \frac{l(l+1)}{r^2}Q_l = 0. \quad (3)$$

Inspired by the example of the Bonnor [7], Weber-Wheeler [8] cylindrical pulse and by our recent work [9], [10], in which time symmetric incoming and outgoing rotating waves are smooth and finite everywhere at all time, we consider, in spherical polar coordinates, the superposition

$$Q_l = B_l\sqrt{\frac{\pi a^3}{2r}}\int_0^\infty (a\omega)^{l+\frac{1}{2}}\, e^{-\omega(a+it)} J_{l+\frac{1}{2}}(\omega r)\, d\omega,$$

where the real amplitude B_l and the characteristic width of the pulse a are constant. We find this integral to yield

$$Q_l(t,r) = B_l 2^l l!\,\frac{(r/a)^l}{\{[(a+it)^2 + r^2]/a^2\}^{l+1}}. \quad (4)$$

Such field is the superposition of rotating waves: it is apparent that for each ω the wave contains the factor

$$e^{im\varphi}e^{-i\omega t} = e^{im(\varphi - \frac{\omega}{m}t)} \quad (5)$$

so that the wave pattern rotates with the rate $\Omega_p = \omega/m$. The rotation and the pulse character of the wave as well as its regularity is easily seen when ψ_{lm} is written explicitly in real terms:

$$\psi_{lm} \sim \frac{P^m_l(\cos\theta)\,\tilde{r}^l\;\cos[m\varphi - \lambda(t,r)]}{[((1+\tilde{r}^2-\tilde{t}^2)^2 + 4\tilde{t}^2]^{(l+1)/2}}, \quad (6)$$

where $\lambda = (l+1)\text{tg}^{-1}\left[2\tilde{t}/(1+\tilde{r}^2-\tilde{t}^2)\right]$, $\tilde{r} = r/a$, and $\tilde{t} = t/a$. It is easy to see, that for high values of l the wave is concentrated near a shell with radius $r^2 = a^2 + t^2$.

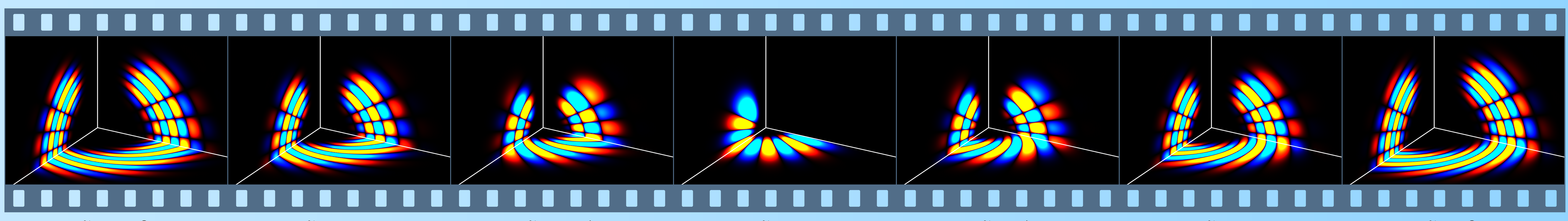

Figure 1. The snapshots of the rotating waves profiles in times $\tilde{t} = -\frac{3}{2}...\frac{3}{2}$ for $l = 17, m = 11$. Waves are localized in the radial direction so that they resemble a falling and rotating shell. Blue color corresponds to negative and yellow to positive values of ψ_{lm}. The wave rotates anticlockwise around the z (vertical) axis. A careful observation reveals that the wave comes inwards in the form of a leading spiral, i.e., with the outside ahead of the inside; at $\tilde{t} = 0$ the spiral structure has changed to a cartwheel but rotation keeps the wave away from the origin; at $\tilde{t} > 0$ the spiral becomes trailing.

Rotating gravitational waves

Field equation for perturbations can be put in the form of Eq. (3) for the scalar field amplitude $Q_l(t,r)$ related to the radial functions $h^{(i)}_{0lm}(t,r)$ and $h^{(i)}_{1lm}(t,r)$ of the odd-parity metric perturbations (7) through the substitution

$$h_{0\,lm} = -\frac{1}{(l-1)(l+2)}\partial_r(r^2 Q_l), \quad (12)$$

$$h_{1\,lm} = -\frac{1}{(l-1)(l+2)}\partial_t(r^2 Q_l). \quad (13)$$

These formulas are valid for $l \geq 2$; in the linear theory in vacuum the dipole odd-parity perturbations ($l = 1$) can be transformed away by a simple gauge transformation [12, 14].

Second order perturbations

In general the second-order metric perturbations $h^{(2)}$ can be obtained by solving the equations

$$G^{(1)}_{\mu\nu}[h^{(2)}] = -G^{(2)}_{\mu\nu}[h^{(1)}, h^{(1)}], \quad (14)$$

where $h^{(i)}$ represent quantities given in (7) with all indices seen explicitly.

However, to determine the influence of gravitational waves on the rotation of local inertial frames at the axis of symmetry we do not need to solve (14) in general. Since terms varying like $\sin 2m\varphi$ or $\cos 2m\varphi$ cannot cause any rotation of the inertial frames on the axis we introduce the average symbol $<>$ and consider the equation

$$G^{(1)}_{\mu\nu}[h^{(2)}] = -< G^{(2)}_{\mu\nu}[h^{(1)}, h^{(1)}] > . \quad (15)$$

To solve these equations we expand both sides in tensor spherical harmonics. The l.h.s. yields a hyperbolic set of equations for $h^{(2)}_0$ and $h^{(2)}_1$ indicating non-instantaneous effects of the first-order terms for general l.

In all our previous work on dragging due to angular momentum of the sources (see, e.g., [3]), the effects were instantaneous at this lowest order. The same situation arises here. Inertial frames at the origin will be influenced primarily by the *dipole* perturbations since all waves behave as r^l there. Now it is well known that for $l = 1$ one can achieve $h_1 = 0$ by an appropriate gauge transformation [11], [14]. The r.h.s. of (15) for axially symmetric component $< G^{(2)}_{t\varphi}[h^{(1)}, h^{(1)}] >$ appears as the only source

$$g(t,r) = \frac{4\pi}{\sqrt{2l(l+1)}\,r}\int_0^\pi < G^{(2)}_{t\varphi} > \partial_\theta Y_{l0}\, d\theta,$$

for the dipole second-order perturbations

$$h^{(2)\prime\prime}_0 - \frac{2}{r^2}h^{(2)}_0 = g(t,r). \quad (16)$$

Its solution $h^{(2)}_0(t,r)$ reads

$$h^{(2)}_0 = -\frac{1}{3r}\int_0^r g(t,r')\,r'^2 dr' - \frac{r^2}{3}\int_r^\infty g(t,r')\,\frac{dr'}{r'}.$$

Frame dragging

For dipole perturbations ($l = 1, m = 0$) near the origin for which only $h^{(2)}_{0\,10} \neq 0$, the general form of the odd-parity metric perturbations (7) yields the metric component $g_{t\varphi}$ in the form

$$-g^{(2)}_{t\varphi} = \sqrt{\frac{3}{4\pi}}h^{(2)}_0(t,r)\sin^2\theta = \omega_0\, r^2\sin^2\theta. \quad (17)$$

The angular velocity of the rotation of an inertial frame of a gyroscope near the origin is then determined by behavior of solution of (16) near origin:

$$\omega_0 = \frac{1}{4\pi}\int_{I\!R^3} G^{(2)}_{t\varphi}[h^{(1)}, h^{(1)}]\,\frac{dx^3}{r^3}. \quad (18)$$

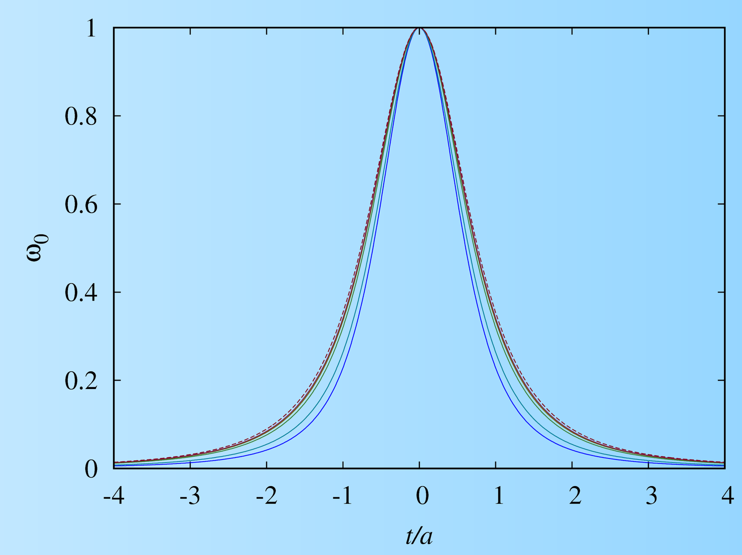

Figure 2. The dependence of normalized angular velocity of the central inertial frame $\omega_0(l,1;t)/\omega_0(l,1;t=0)$ on the parameter $l = 2, 3, 10, 20, 30$ (from inside to out). Also the function $(1+\tilde{t}^2)^{-3/2}$ is shown as a dashed line to indicate the limit for large l.

Although $G^{(2)}_{t\varphi}[h^{(1)}, h^{(1)}]$ has a complicated structure, we obtained the angular velocity ω_0 in the closed form

$$\omega_0(t) = \frac{\tilde{B}^2_l}{2\pi}\,\frac{m\,(l+1)\,(l+2)}{a\,(l+3)\,l}\times \left[\left(U_l - V_l\tilde{t}^{\,2}\right)\tilde{I}^2_{l+3}(\tilde{t}) + \left(U_l + V_l\tilde{t}^{\,2}\right)I^1_{l+3}(\tilde{t})\right], \quad (19)$$

where

$$U_l = \left(2\,l^5 + 7\,l^4 + 4\,l^3 - 7\,l^2 + 24\,l + 36\right), \quad (20)$$
$$V_l = 3\left(l^4 + 2\,l^3 + 3\,l^2 + 8\,l + 12\right).$$

$$I^1_{l+3} = \frac{(1+\tau^2)^{-l-4}}{2^{3l+6}(l+2)!}\left(\frac{(\tau^2+1)^2}{\tau}\frac{d}{d\tau}\right)^{l+1}\Pi_1, \quad (21)$$

$$\Pi_1 = \frac{(\tau^2+1)^3}{\tau^3}\text{tg}^{-1}\tau + \frac{\tau^4 - 1}{\tau^2},$$

$$\tilde{I}^2_{l+3} = \frac{(1+\tau^2)^{-l-4}}{2^{3l+6}(l+2)!}\left(\frac{(\tau^2+1)^2}{\tau}\frac{d}{d\tau}\right)^{l}\Pi_2, \quad (22)$$

$$\Pi_2 = 3\frac{(\tau^2+1)^5}{\tau^5}\text{tg}^{-1}\tau + \frac{\tau^4 - 1}{\tau^4}(3\tau^4 + 14\tau^2 + 3).$$

Observing stars

If we assume a telescope pointed towards the star's initial position at $T \to -\infty$, the quantities $\delta\theta$ and $\sin\theta\delta\varphi$ proportional to star's coordinates on telescope's photographic plate can be described by a simple formula

$$\frac{\delta\varphi}{\Delta\varphi} + i\frac{\delta\theta}{\Delta\theta} = \frac{i^l\, e^{im\varphi}}{(1 + i\frac{T}{a})^{l+2}}. \quad (23)$$

We see that the same image is replicated for all stars (Figure 3). Depending on the star's position the image is rotated by $e^{im\varphi}$ and then scaled by factors $\Delta\theta \sim mP^m_l(\cos\theta)/\sin\theta$ in the latitudinal and by $\Delta\varphi \sim P'^m_l(\cos\theta)$ in the longitudinal direction. Surprisingly, the images are time-symmetric with the maximal deflection occurring at $T = 0$ despite the fact that the deflection is calculated using retarded integrals.

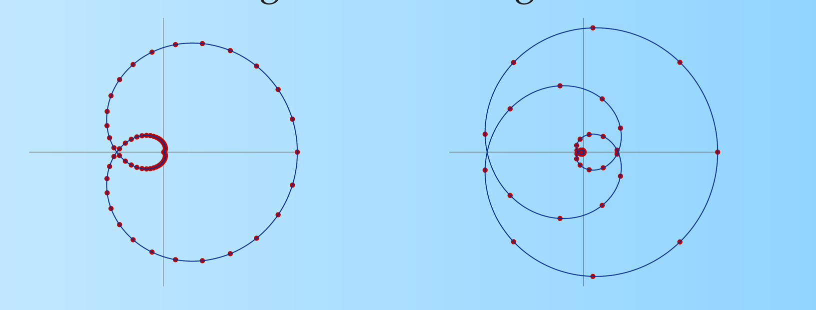

Figure 3. Since light from distant stars is influenced by the gravitational waves the observed positions of the stars change. An observer at the origin can record the apparent position of the stars on the celestial sphere on a photographic plate. When appropriately scaled and rotated, the trajectories of all stars are the same. A star starts at the origin of the plate ($x = y = 0$ in the planes above) and moves along closed trajectories the structure of which becomes more complicated with increasing l, trajectories for $l = 3$ (left) and $l = 13$ (right) are shown. At the moment of time symmetry, $\tilde{t} = 0$, the image is located at maximal value of x (with $y = 0$). Together with the trajectory, positions at time $\tilde{t} = 0, \pm 0.05, \pm 0.1, ...$ are shown as circles.

References

[1] A. Einstein, Vierteljahrsschrift für gerichtliche Medizin und öffentliches Sanitätswesen **44**, 37 (1912).
[2] J. Barbour and H. Pfister, eds., *Mach's Principle: From Newton's Bucket to Quantum Gravity*, vol. 6 of *Einstein studies* (Birkhäuser, Boston, 1995).
[3] J. Bičák, J. Katz, and D. Lynden-Bell, Phys. Rev. D **76**, 063501 (2007).
[4] C. Schmid, Phys. Rev. **D79**, 064007 (2009).
[5] J. Bičák, J. Katz, T. Ledvinka, and D. Lynden-Bell, Phys. Rev. D **85**, 124003 (2012).
[6] J. Katz, D. Lynden-Bell, and J. Bičák, Class. Quantum Grav. **15**, 3177 (1998).
[7] W. B. Bonnor, J. Math. Mech. **6**, 203 (1957).
[8] J. Weber and J. A. Wheeler, Rev. Mod. Phys. **29**, 509 (1957).
[9] J. Bičák, J. Katz, and D. Lynden-Bell, Class. Quantum Grav. **25**, 165017 (2008).
[10] D. Lynden-Bell, J. Bičák, and J. Katz, Class. Quantum Grav. **25**, 165018 (2008).
[11] T. Regge and J. A. Wheeler, Phys. Rev. **108**, 1063 (1957).
[12] F. J. Zerilli, Phys. Rev. D **2**, 2141 (1970).
[13] H. Nakano and K. Ioka, Phys. Rev. D **76**, 084007 (2007).
[14] J. Bičák, Czech. J. Phys. **B29**, 945 (1979).